Occupant restraint optimisation in frontal crash to mitigate the risk of submarining in out-of-position situation

Olivier Richard, Jérôme Uriot, Xavier Trosseille, Marcin Sokolowski*

Abstract Submarining can be described as a slipping of the lap-belt above the iliac spines of the occupant during frontal crash. This can cause very serious injuries.

The goal of this study is to compare different finite element (FE) simulations performed with a biofidelic THOR dummy in a real seat with similar Post Mortem Human Subject tests. This dummy was obtained by modifying a standard FE THOR model.

In the first stage, two configurations of tests were defined: the first one was to correctly restrain the occupant; and the second was to observe the submarining. Three PMHS tests were performed for each configuration. They are presented in a companion paper (Uriot et al., 2015). For the "non-submarining" configuration, the occupants were well restrained. For the second configuration, submarining was observed.

In the second stage, to decrease the risk of injury in the "submarining" configuration, a FE study with the biofidelic THOR dummy was performed. The enhanced restraint system was composed of a double lap-belt pretension and a double lap-belt load limiter. Three new PMHS tests – presented in the companion paper – were performed. A good correlation level was observed between PMHS and biofidelic THOR dummy test results regarding the risk of submarining.

Keywords frontal crash, lap belt, PMHS, submarining, THOR.

I. INTRODUCTION

Submarining is a complex phenomenon that can occur during frontal crash. It's described as a sliding of the lap-belt above the iliac spines of the occupant (Luet et al., 2012 [1]) (Fig. 1). It is restricted here to the belt being positioned correctly at time zero.

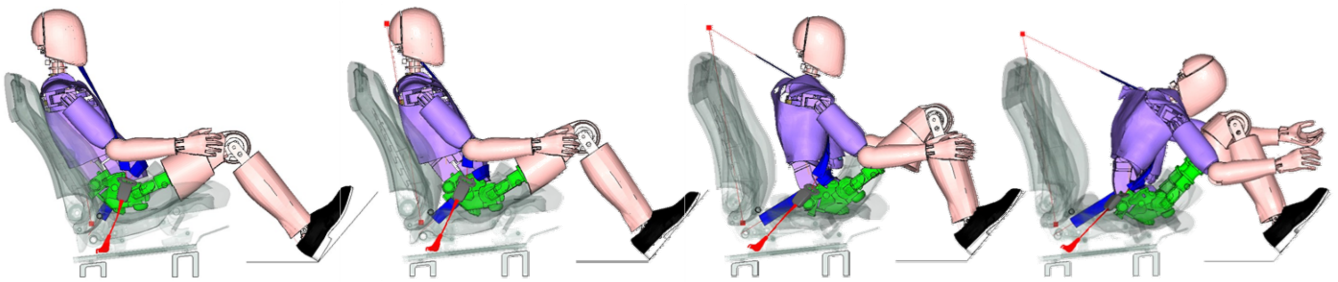

Fig. 1. Illustration of the submarining phenomenon with the THOR dummy in OOP.

One of main causes of severe abdominal injuries (AIS 3+) in front crash for belted occupants noticed by Lamielle et al. (2006) [2] is submarining.

Three specific parameters can be mentioned to explain the reasons of submarining phenomenon. The first is the initial position of the occupant. Leung et al. (1979) [3] indicate that, the more the pelvis is initially rearward inclined, the higher the risk of submarining occurring. When Hx is defined as the H-Point coordinate in x of the occupant (nominal or standard position) (Fig. 2), an out-of-position (OOP) is defined as a position which differs

*O. Richard is Safety Engineer at the Department of Research and Development, Faurecia Automotive Seating, France (phone: +33-1-69785099, e-mail: olivier.richard@faurecia.com). J. Uriot is Research Engineer at Department of Biomechanics, CEESAR, France. X. Trosseille is Expert in Biomechanics at LAB PSA Peugeot Citroën Renault, France. M. Sokolowski is FEA Engineer at the Department of Research and Development, Faurecia Automotive Seating, Poland.

from the standard position (Fig. 3). When the occupant has his pelvis closer to the front of the seat (Hx +X mm), it increases the initial pelvis angle, and it also increases the risk of observing the submarining of the occupant.

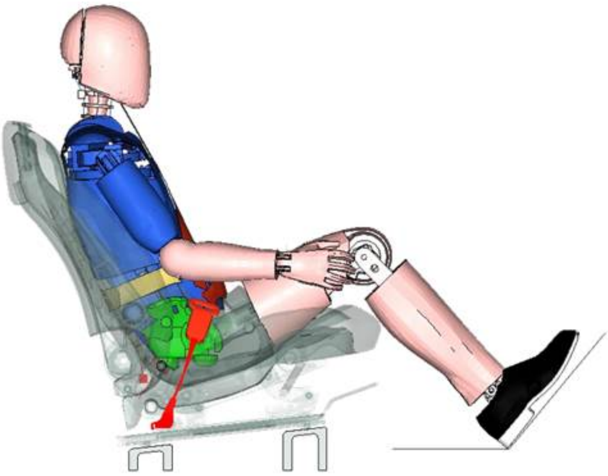

Fig. 2. Standard position: low risk of submarining (Hx)
Initial pelvis position: green

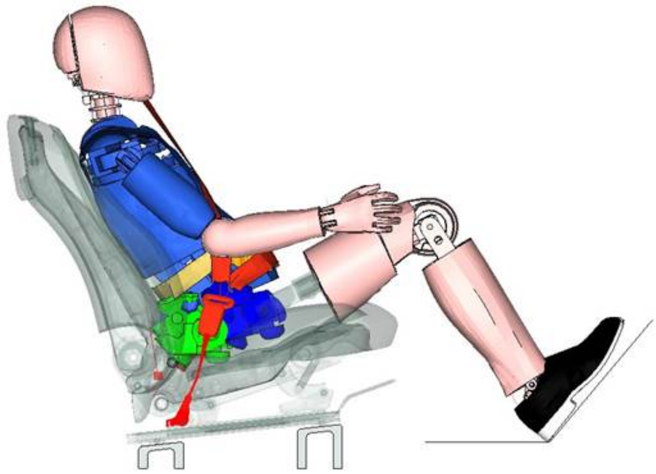

Fig. 3. OOP: high risk of submarining (Hx +100 mm)
New pelvis position: blue

The second parameter is the relative position between the lap-belt and the occupant (i.e. position of the lap-belt anchorages). Tarrière (1973) [4] points out that the initial angle of the lap belt has to be more vertical in order to reduce the risk of submarining. The risk of submarining is therefore influenced by the orientation of the lap-belt, and by the position of the lap belt anchorages. A rear anchorage in x of the lap-belt will induce a lap-belt more horizontal, and thereby increasing the risk of submarining.

The third parameter is the type of restraint system. Haland et al. (1991) [5] indicate that the risk of submarining increasing with belt slack. The type of restraint system and, in particular, the presence or not of a pretensioner, is therefore a key factor to reduce the risk of submarining. A pretension device reduces the slack between the occupant and the seat belt, which then allows to the seat belt to be more effective in correctly restraining the occupant. The risk of submarining is therefore reduced by the presence of pretensioner.

From January 2015, submarining is assessed by Euro NCAP using a 05th percentile dummy for the front and rear passengers of the car during a frontal full width crash test at 50km/h. After this test, a negative modifier to the "Knee, Femur & Pelvis" body part is applied when submarining occurs (Euro NCAP Assessment Protocol – AOP 7.0.1) [6]. Submarining is now a phenomenon used to assess the safety performance of the vehicles.

The THOR dummy, for which the development is almost finalized, will be the dummy used during the front crash for the regulation tests and for the consumer tests as Euro NCAP. We estimate that this new dummy will be introduced in 2020 for use during Euro NCAP front crashes (Euro NCAP 2020 Roadmap, March 2015) [7].

The purpose of this study was to develop and validate a FE biofidelic THOR dummy with a high biofidelity level regarding the risk of submarining. For this, an existing FE THOR dummy was modified with the help of PMHS tests realised on rigid seats (Luet et al. [1]). Afterwards, a comparison was done between the results achieved during PMHS tests on real seats (Uriot et al., 2015 [8]) with FE results obtained with the FE biofidelic THOR dummy. To cover a large scope of use with the FE biofidelic THOR dummy, the quality level of this tool was assessed for two significant and different behaviours: one configuration with submarining; and one configuration without submarining.

Finally, the restraint of the occupant was optimised for the configuration where submarining was observed with the help of the FE biofidelic THOR dummy, and Uriot et al. [8] performed new PMHS tests to assess the level of predictivity of this new FE tool.

II. METHODS

In this study, numerical and physical methodologies were used to achieve the objectives. They are presented in Fig. 4.

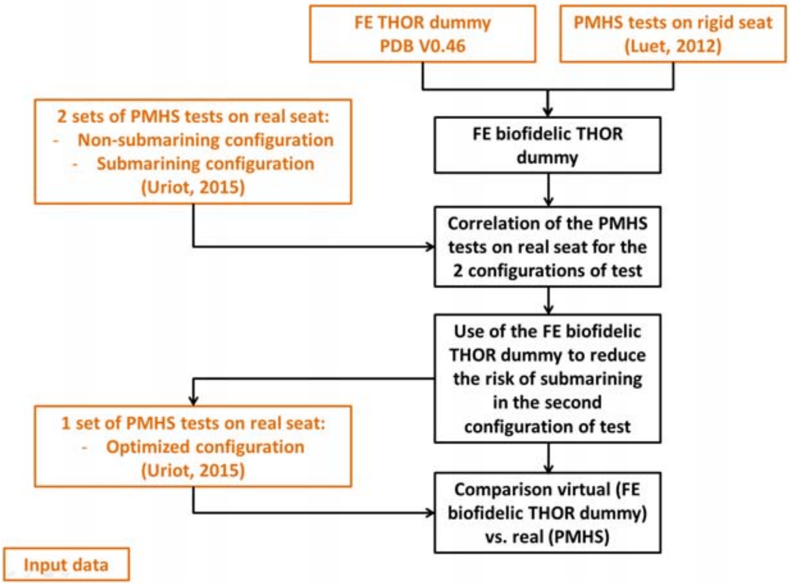

Fig. 4. Flowchart of the steps performed during the study.

Modification of the existing FE THOR dummy to generate the FE biofidelic THOR dummy

The existing FE THOR dummy was provided by the Partnership for Dummy technology and Biomechanics (PDB) in version V0.46.

The initial general characteristics of this dummy are presented in Appendix 1 of this document.

✓ ***FE biofidelic THOR dummy***

The target was to adjust the existing FE THOR dummy in order to correlate the behaviour of the PMHS observed during the nine tests of Luet et al. [1] on rigid seat.

During this test campaign, Luet et al. [1] particularly studied the ability of PMHS to submarine according to three different restraint systems. The restraint system was made-up of two separated straps to easily manage the FE modelling. The thoracic belt part was comprised of a retractor for the high point, and a fixed point for the lower anchorage. The pelvic belt part was comprised of two retractors: one for both side of the occupant. These three retractors were blocked in rotation. A defined length of webbing on the spool of the retractor allowed to vary the overall stiffness of the webbing.

Table 1 presents the different parameters used for the tests campaign of Luet et al. [1].

TABLE 1
PARAMETERS OF THE DIFFERENT CONFIGURATIONS TESTED BY LUET ET AL. [1]

	Configuration 1	Configuration 2	Configuration 3
Cushion angle	0°	0°	5°
Test velocity	11 m/s	14 m/s	14 m/s
Position of the belt anchorages	Rear	Front	Rear
Strap length within the lap-belt retractors	800 mm	600 mm	600 mm
Position of the footwell	Front	Front	Rear
PMHS	631 / 632 / 633	634 / 635 / 636	637 / 638 / 639

✓ **Description of the sled model with rigid seat**

The sled model corresponds to the environment used by Luet et al. [1] to perform the nine PMHS tests. It was mainly tuned regarding the level of correlation of the belt forces. The cushion was completely non-deformable; it was therefore modelled with rigid elements. The sled model is presented in Fig. 5, and the seat belt model is presented in Fig. 6.

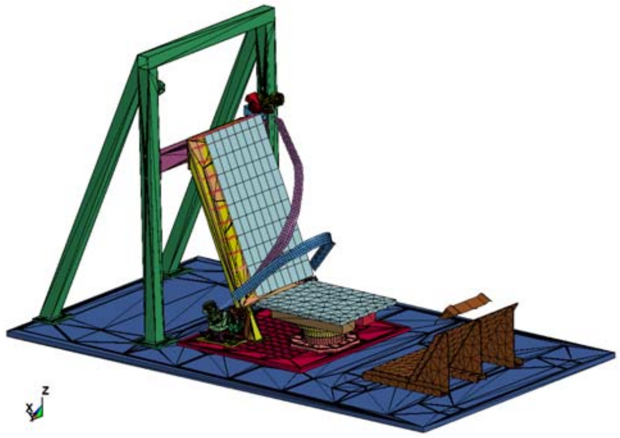

Fig. 5. Sled model with rigid seat.

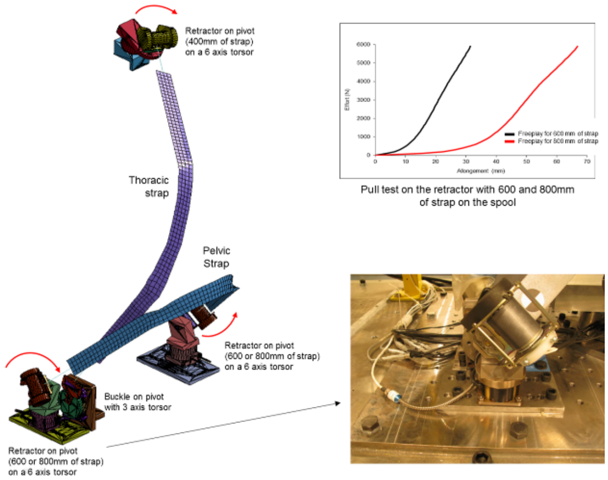

Fig. 6. Modeling of the four-point belt system.

✓ ***Main modifications of the FE biofidelic THOR dummy***

One of the main issues of the initial FE THOR dummy was its inability to obtain similar pelvis rotation to those recorded during PMHS tests on rigid seat. The objective of the principal modifications was therefore to increase the rotation of the pelvis and thorax. Fig. 7 presents the parts on which modifications were performed.

The main modifications were:

- elongation of the lumbar spine and modification of the material.
- Cancellation of the contact between the lumbar spine and the abdomen support.
- Cancellation of the hard contact between the lower part of the thorax and the abdomen support.
- Modification of the deformable part of the abdomen support in order to soften the contact between the lower part of the thorax and the abdomen.
- Cancellation of the contacts between the femurs and the internal deformable parts of the pelvis in order to soften the rotation stiffness in the hips area.

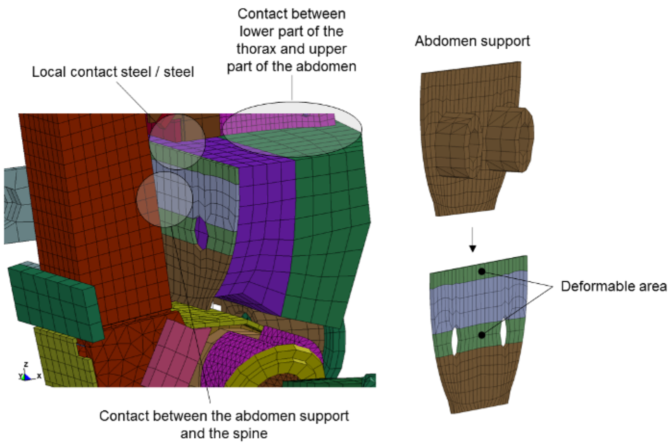

Fig. 7. Abdomen area of the FE THOR dummy.

All the deformable materials were adjusted in order to improve the biofidelity of the new FE THOR dummy, to obtain a tool that was numerically stable and to reduce the calculation duration. The shape of the pelvis was also modified to improve the coupling between the lap-belt and pelvis, and to tune the ability of the dummy to submarine. The stiffness of the elements was adjusted to mimic the behaviour of the pelvis observed during the PMHS tests of Luet et al. [1]. A specific focus was done regarding the loading of the pelvis by the seat cushion and the sliding between the lap-belt and the deformable parts of the pelvis. The mechanical structure of the dummy was not modified. These modifications are totally feasible on a physical dummy.

These modifications are presented Fig. 8.

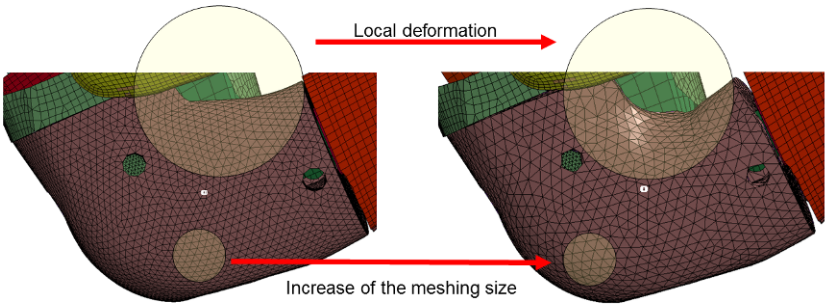

Fig. 8. Modification of the shape of the pelvis and increase of the meshing size.

Virtual testing on real seat

The seat model used for this study was a model of a real seat already validated and correlated with previous sled tests performed with the standard dummies used for front crash (Fig. 9).

To correlate the different PMHS tests performed by Uriot et al. [8], a model of the sensor between the seat and the seat support was created. This sensor was present for the physical tests (Fig. 10 and Fig. 11).

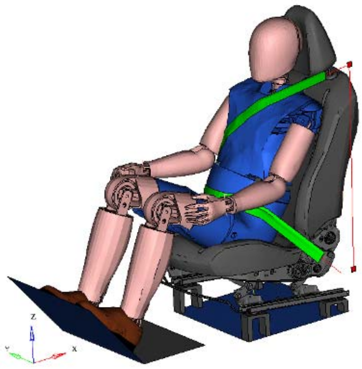

Fig. 9. Real seat model used for the virtual testing.

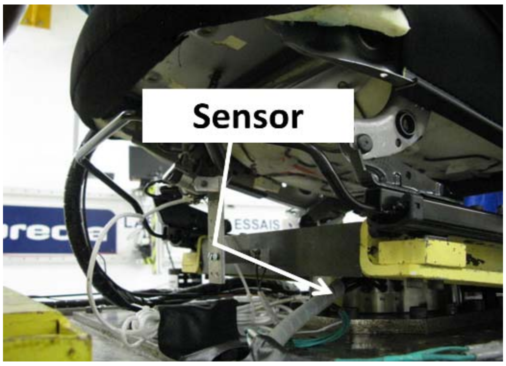

Fig. 10. Interface between the seat and the sled: a specific sensor was fixed between the sled and the seat to measure the load applied during the front crash.

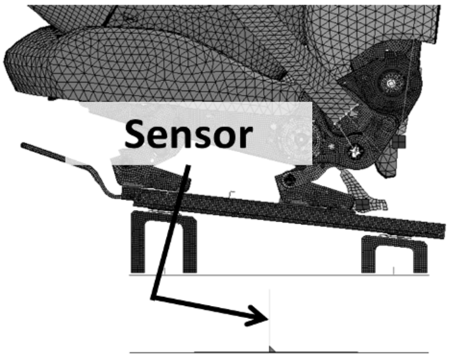

Fig. 11. A simplified modelling of the montage was set-up to correlate the mass used during the tests.

To achieve a reliable comparison between the PMHS tests results and the virtual tests performed with the FE biofidelic THOR dummy, the initial conditions observed and measured during the PMHS tests on real seat of Uriot et al. [8] were duplicated in the FE model:

- ✓ H-Point coordinates in x and z.
- ✓ Initial pelvis angle – As described by Uriot et al. (2006) [9], the line used to orientate the pelvis is the H-Point – iliac crest line. This line was recorded before the different PMHS tests (Fig. 12 and Fig. 13).
- ✓ Position of the belt – The coordinates of the belt measured during the experimental testing were used and the belt in FEA was repositioned with these coordinates.
- ✓ Position of the thorax.
- ✓ Position of the femur.

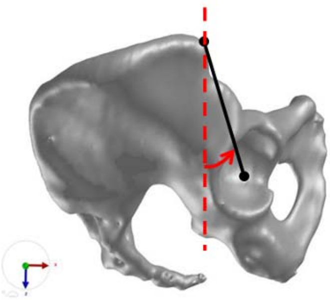

Fig. 12. Initial pelvis angle (H-Point – iliac crest line) measured with the PMHS.

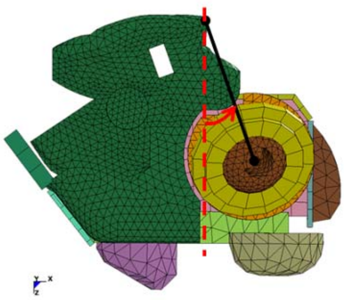

Fig. 13. Initial pelvis angle adjusted for the FE THOR dummy to correlate the initial position of the PMHS.

Experimental testing with PMHS on real seat

Nine PMHS tests were performed by Uriot et al. [8]. These tests are fully detailed in the companion paper.

The nine PMHS tests were split in 3 sets of 3 tests:

- One series of 3 tests to restrain correctly the PMHS (configuration A):
  - Standard restraint system;
  - Standard position of the occupant;
  - Standard lap-belt anchorages.

- One series of 3 tests to observe the submarining of the PMHS (configuration B):
  - OOP of 60 mm: Hx +60 mm → High initial pelvis angle → high probability of submarining;
  - No pretension → Standard slack between lap-belt and occupant → High probability of submarining;
  - Rear position in x for the lap belt anchorages → Lap-belt more horizontal → High probability of submarining.

- One series of 3 tests to reduce the risk of submarining and injuries after the optimisation of the restrain system for the configuration B (configuration C):
  - OOP of 60 mm: Hx +60 mm → High initial pelvis angle → High probability of submarining;
  - Rear position in x for the lap-belt anchorages → Lap belt more horizontal → High probability of submarining;
  - Enhanced restraint system (presented after).

One unique front crash pulse was used for all the tests. The final velocity is 14 $m.s^{-1}$. The velocity and accelerations are presented in Appendix 2.

FEA Sensitivity study to reduce the risk of submarining for configuration B (configuration C)

To reduce the risk of submarining and injuries in configuration B, different FEA investigations were performed. For some of the iterations, lap-belt load limiters were used to reduce the force applied on the pelvis, and especially on the iliac crests, to minimise the risk of fracture of these parts observed during initial tests. Lap-belt pretensioners were used for some of the other iterations, to reduce the slack within the lap-belt, and to minimise the risk of submarining (Haland et al. [5]).

All the iterations performed are presented in Appendix 3.

III. RESULTS

FE biofidelic THOR dummy

✓ **Comparison of PMHS, FE THOR dummy and FE biofidelic THOR dummy responses on rigid seat**

The next curves (Fig. 14) present for the 3 series of tests performed by Luet et al. [1], the comparison between the PMHS corridor, the initial FE THOR dummy and FE biofidelic THOR dummy responses regarding the pelvis rotation.

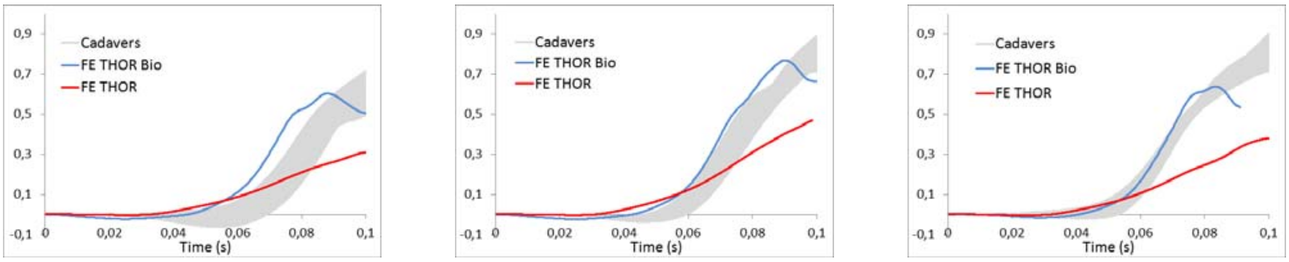

Fig. 14. Comparison of pelvis rotation (rad) between PMHS tests and FE simulations for the 3 configurations.

We observed a clear improvement of the pelvis rotation with the FE biofidelic THOR dummy.

The other results are presented in Appendix 4.

- ✓ **Ability to submarine**

With the modifications described in the previous chapter on the FE biofidelic THOR dummy, we reached the same propensity to submarine with the FE biofidelic THOR dummy as with the PMHS. Table 2 summarises the results achieved. The timing of submarining used in Table 2 is the start of the sliding between lap-belt and the pelvis. This timing was determined with the video analysis and corresponds also to the drop of lap-belt force.

Configuration 3 generated the earliest submarining, followed by configuration 1. Finally, configuration 2, with one submarining case out of 3, was the configuration best able to limit this phenomenon.

This order was also verified with the new FE biofidelic THOR dummy.

TABLE 2

COMPARISON REGARDING TIME OF SUBMARINING FOR THE PMHS AND THE FE BIOFIDELIC THOR DUMMY

		Configuration 1			**Configuration 2**			**Configuration 3**		
PMHS		631	632	633	634	635	636	637	638	639
submarining occurrence (ms)	**PMHS**	92	80	96	w/o	w/o	80	65	75	71
	FE THOR Bio		87			89			83	

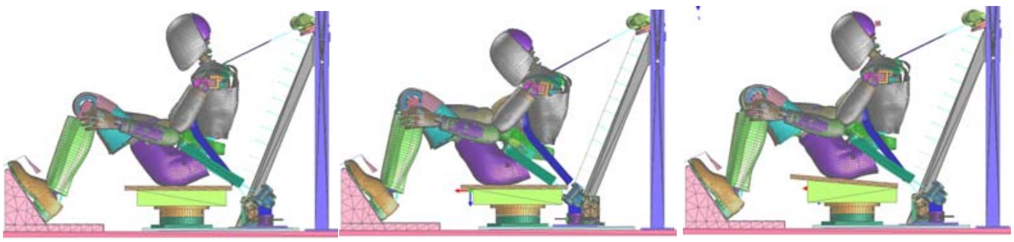

Results of the PMHS tests on real seat according to non-submarining configuration (configuration A)

A synthesis of the results is presented in Table 3. The full, detailed results are presented in a companion paper by Uriot et al. [8].

TABLE 3

RESULTS ACHIEVED WITH PMHS FOR CONFIGURATION A

Tests	PMHS	H-pt position	Tracks	Pretension	Belt buckle	Results
IRIS 32	649	Hx	Nominal	With	Nominal	No submarining
IRIS 33	650	Hx	Nominal	With	Nominal	No submarining (fracture of one iliac spine about 70 ms)
IRIS 34	648	Hx	Nominal	With	Nominal	No submarining

Comparison of real and virtual tests according to non-submarining configuration (configuration A)

For this series of tests, the submarining phenomenon was not observed for the 3 PMHS. The results achieved with the FE biofidelic THOR dummy were similar to the results obtained with the PMHS during physical tests on real seat (Fig. 15).

The quality of the models was assessed with the WIFac method [10]. The results are presented in Appendix 4.

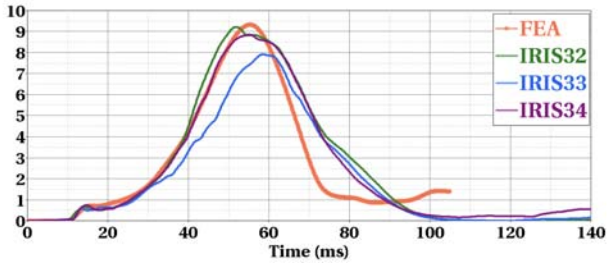

External lap-belt force (kN)

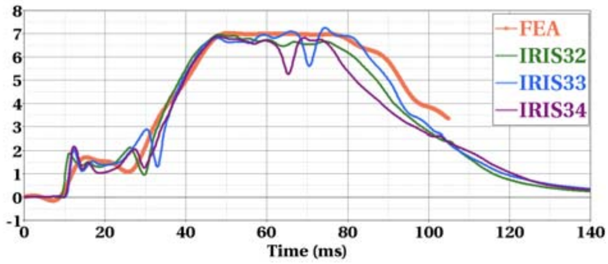

Shoulder-belt force (kN)

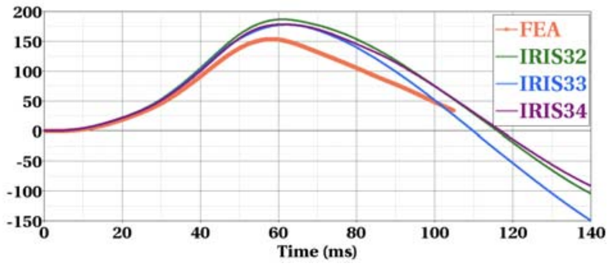

Pelvis x displacement (mm)

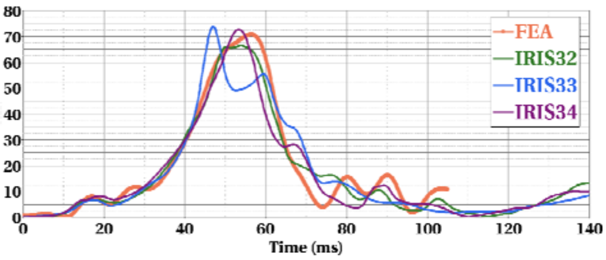

Pelvis acceleration (g)

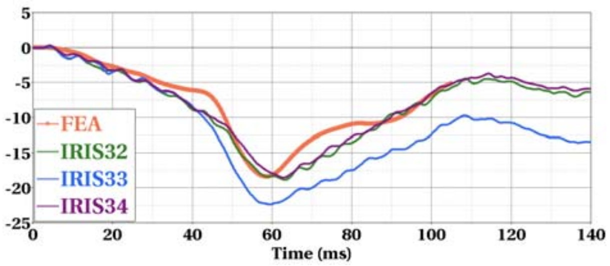

Seat crossmember x displacement (mm)

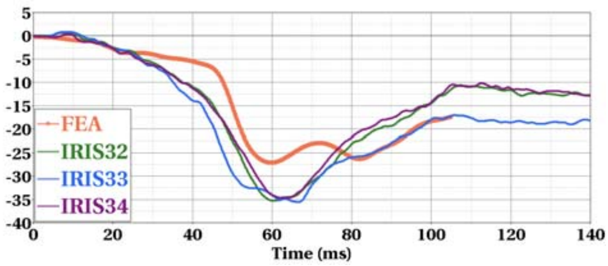

Seat crossmember z displacement (mm)

Fig.15. Comparison between PMHS and FE biofidelic THOR dummy responses for configuration A.

Results of the PMHS tests on real seat according to submarining configuration (configuration B)

A synthesis of the results is presented in Table 4. The full, detailed results are presented in a companion paper by Uriot et al. [8].

TABLE 4
RESULTS ACHIEVED WITH PMHS FOR CONFIGURATION B

Tests	PMHS	H-pt position	Tracks	Pretension	Belt buckle	Results
IRIS 29	653	Hx +60 mm	Nominal +50 mm	Without	Nominal -50 mm (initial position)	Submarining (two iliac spines broken about 58 ms)
IRIS 30	652	Hx +60 mm	Nominal +50 mm	Without	Nominal -50 mm (initial position)	Submarining (two iliac spines broken about 50 ms)
IRIS 31	651	Hx +60 mm	Nominal +50 mm	Without	Nominal -50 mm (initial position)	Submarining (two iliac spines broken about 48 ms)

Comparison of real and virtual tests according to submarining configuration (configuration B)

The comparison between virtual and real tests was done only for the tests IRIS 30 and IRIS 31. The data of the test IRIS 29 were not correctly recorded and therefore a comparison was not possible between this test and the result of the FE simulation.

The comparison was relevant between 0 and 50 ms because iliac spines fractures were observed at approximately 50ms for all of the different PMHS.

The level of correlation during this time corridor was completely satisfactory. For all of the curves presented below, similar behaviours between FE biofidelic THOR dummy and the 2 PMHS tested were observed (Fig. 16). The quality of the models was assessed with the WIFac method [10]. The results are presented in Appendix 5.

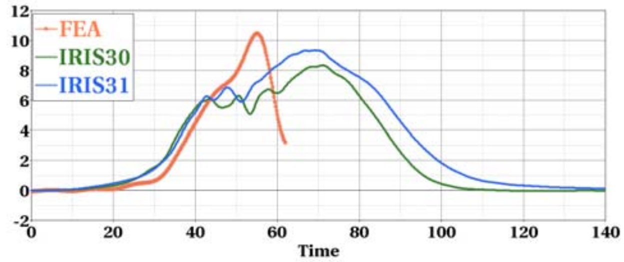

External lap-belt force (kN)

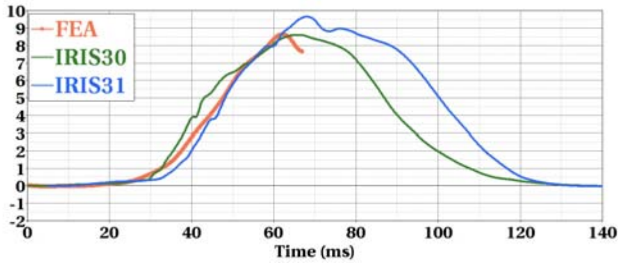

Shoulder-belt force (kN)

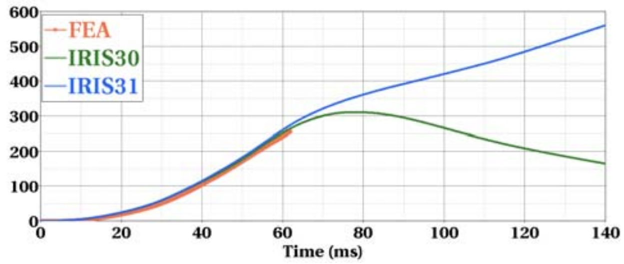

Pelvis x displacement (mm)

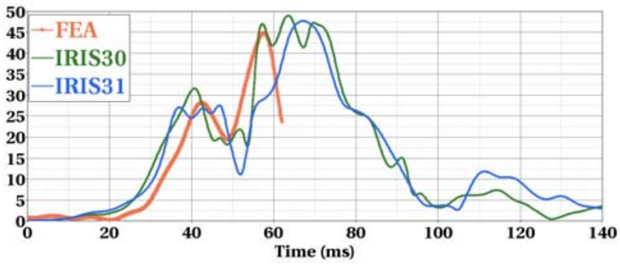

Pelvis acceleration (g)

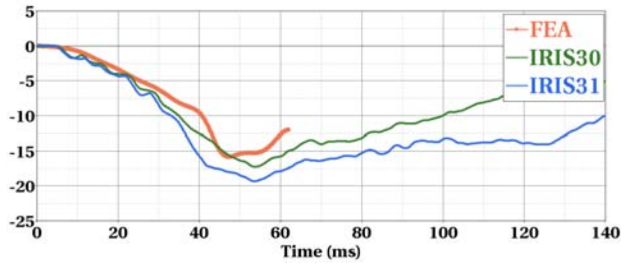

Seat crossmember x displacement (mm)

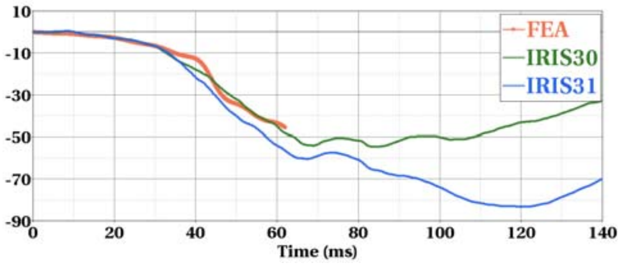

Seat crossmember z displacement (mm)

Fig. 16. Comparison between PMHS and FE biofidelic THOR dummy responses for configuration B.

Result of the FEA sensitivity study to optimise the occupant restraint using the FE biofidelic THOR dummy in configuration B (configuration C)

For this FEA campaign, the dummy was in OOP (Hx +60 mm), and the lap-belt anchorages were still in a rearward position. This meant that the occupant was still in a favourable situation to submarine.

The following trends were observed with the sensitivity study performed:

- ✓ No pretensioner (initial iteration): Submarining at around 55 ms
- ✓ One pretensioner (shoulder or belt buckle): Submarining at around 60 ms
- ✓ One pretensioner + one lap-belt load limiter: Submarining at around 65 ms
- ✓ Two pretensioners (external and internal lap-belt): Submarining at around 70 ms
- ✓ Two pretensioners + one lap-belt load limiter: Submarining at around 75 ms
- ✓ Two pretensioners + two lap-belt load limiters: No submarining

A final FE iteration with the following restraint system was performed:

- 2 lap-belt pretensioners;
- 2 lap-belt load limiters with a force level of 4 kN;
- A shoulder load limiter with a force level of 6 kN.

Due to an issue in obtaining this configuration with standard parts for the physical tests, it was decided to separate the belt parts at the belt buckle area, and to work with two separated straps (Fig. 17).

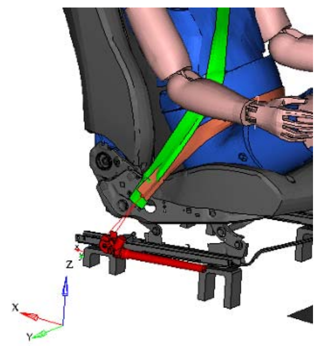

Fig. 17. Separated belts at belt buckle area.
Green: thoracic part / orange: lap-belt part

With the configuration described previously, we still reached a configuration without submarining. Fig. 18

shows no drop of force within the lap belt. This means that there is no submarining of the dummy.

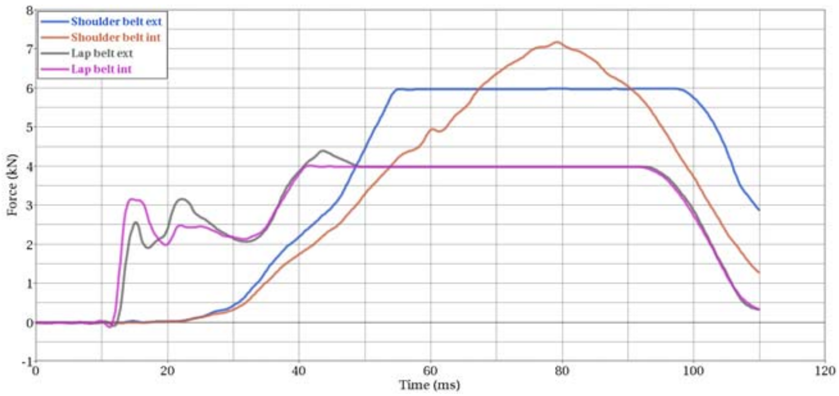

Fig. 18. No submarining with the new restraint configuration.

Results of the PMHS tests on real seat according to optimised configuration

The configuration validated in FEA was prototyped and assessed with PMHS. A synthesis of the results is presented in Table 5. The full, detailed results are presented in a companion paper by Uriot et al. [8].

TABLE 5
RESULTS ACHIEVED WITH PMHS FOR CONFIGURATION C

Tests	PMHS	H-pt position	Tracks	Pretension	Belt buckle	Results
IRIS 39	659	Hx +60 mm	Nominal +50 mm	With	Nominal -50 mm (initial position)	No submarining
IRIS 40	657	Hx +60 mm	Nominal +50 mm	With	Nominal -50 mm (initial position)	No submarining (fracture of one iliac spine about 94 ms)
IRIS 41	658	Hx +60 mm	Nominal +50 mm	With	Nominal -50 mm (initial position)	No submarining

PMHS MS657 was the heaviest of the 3 PMHS tested in this campaign. His mass was 90 kg (54 kg for PMHS MS659 and 69 kg for PMHS MS658).

Comparison of real and virtual tests according to optimised configuration

Due to the difference of anthropometry between MS657 and (MS659 + MS658), 2 types of curves were observed regarding the different criteria used to compare the virtual and experimental results. Except for the seat crossmember displacements (front part of the seat cushion), the FEA curves were within the corridor composed by the three curves. The differences can be explained by the mass differences between the PMHS used and by the fact that lap-belt load limiters were used. The use of an independent lap-belt with load limiter induces a loading duration within the lap-belt very sensitive to the mass of the occupant. All the results are presented in Fig. 19.
The quality of the models was assessed with the WIFac method [10]. The results are presented in Appendix 5.

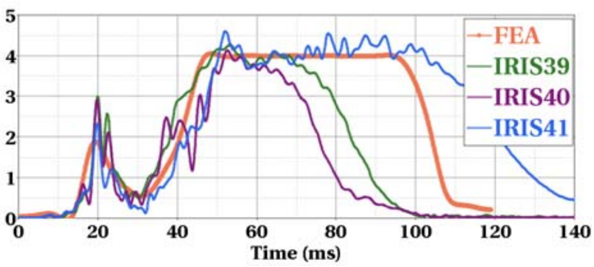

External lap-belt force (kN)

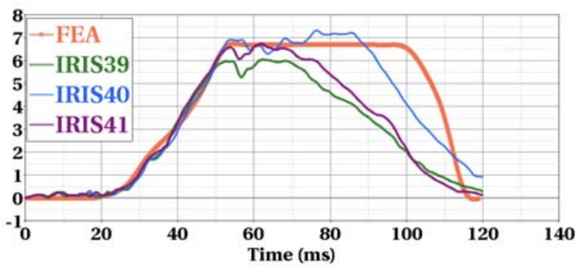

Shoulder-belt force (kN)

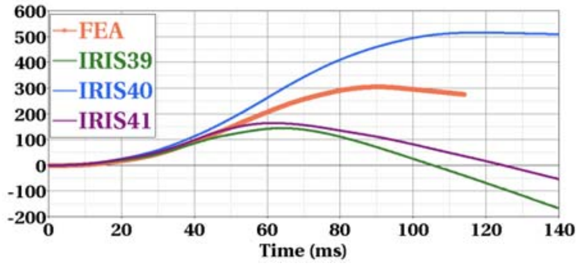

Pelvis x displacement (mm)

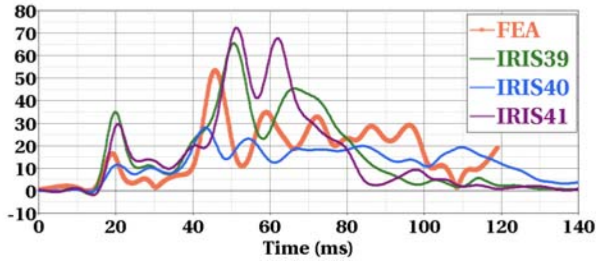

Pelvis acceleration (g)

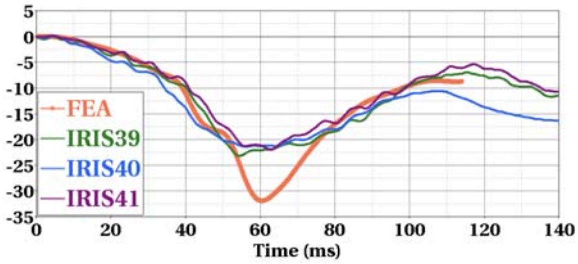

Seat crossmember x displacement (mm)

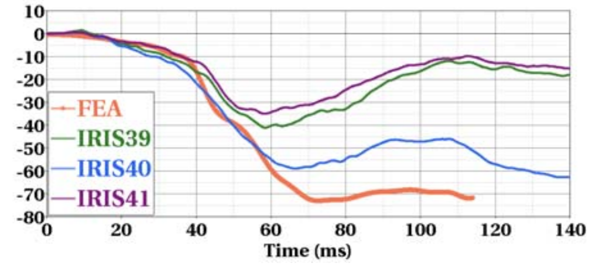

Seat crossmember z displacement (mm)

Fig. 19. Comparison between PMHS and FE biofidelic THOR dummy responses for configuration C.

IV. DISCUSSION

The FE biofidelic THOR dummy developed with nine PMHS tests performed on a rigid seat by Luet et al. [1] was used in comparison with 3 series of different PMHS tests on a real seat (Uriot et al. [8]). The results are satisfactory for both biomechanical criteria measured and the prediction of submarining risk.

For this type of seat architecture, the correlation level obtained allows us to conclude that this new FEA tool can be used to assess the risk of submarining for human beings during seat development.

At this step of the study, we don't know if this correlation level can be equivalent for other types of seat architectures, i.e. stiffer or softer seat cushions. However, the FEA dummy was initially modified to correlate the tests with PMHS on a rigid seat. This rigid seat can be compared to a real seat with a stiff cushion, and during the project a comparison was made for a situation of submarining. This situation can be obtained for a real seat with a very soft cushion. Finally, a large scope of application was used to validate this FEA tool.

The modifications were made to improve the biofidelity regarding the risk of submarining. As presented, the modifications influenced the pelvis rotation and will probably change also head and chest responses. The biofidelity of these FE dummy parts were not assessed during the study.

The optimisation phase performed to reduce the risk of submarining for configuration B was possible with a complete restraint system modification. With this modification, we avoid severe injuries of the PMHS and especially iliac spines fractures.

V. CONCLUSIONS

The new FEA tool developed during this study presents a high level of prediction regarding the risk of submarining for PMHS. It can be easily used for seat development for this specific risk, like the FEA tools that are currently used for validation, such as the Hybrid 3 or Hybrid 2 dummies. The modifications applied to the FEA dummy could be the basis for some potential modifications of the real dummy to improve its biofidelity regarding the submarining phenomenon.

VI. ACKNOWLEDGEMENTS

The authors would like to acknowledge Stéphane Léger, Steeve Lainé and Kurt Driscoll from Faurecia Automotive Seating for providing support in this project.

VII. References

[1] Luet et al. Kinematics and dynamics of the pelvis in the process of submarining using PMHS sled tests. *Stapp Car Crash Journal*, 2012, Vol. 56: pp. 411-442.

[2] Lamielle et al. Abdominal injury patterns in real frontal crashes: influence of crash conditions, occupant seat and restraint systems. *Proceedings of the 50th A.A.A.M. Conference*, 2006, Chicago (USA).

[3] Leung et al. A Comparison between Part 572 Dummy and Human Subject in the problem of Submarining. *Proceedings of the 23rd Stapp Car Crash Conference*, 1979, San Diego (USA), pp. 677-719.

[4] Tarrière C. Proposal for a Protection Criterion as Regards Abdominal Internal Organs. *Proceedings of the 17th A.A.A.M. Conference,* 1973, Oklahoma City (USA), pp. 371-382.

[5] Haland et al. Seat Belt Pretensioners to Avoid the Risk of Submarining – A Study of Lap belt Slippage Factors. *13th International Conference on Experimental Safety Vehicles,* Paris (France), 1991, pp. 1060-1068.

[6] Euro NCAP Assessment Protocol – AOP 7.0.1. Internet: http://euroncap.blob.core.windows.net/media/1565/euro-ncap-assessment-protocol-aop-v-701.pdf.

[7] Euro NCAP 2020 Roadmap, March 2015. Internet: http://euroncap.blob.core.windows.net/media/16472/euro-ncap-2020-roadmap-rev1-march-2015.pdf.

[8] Uriot et al. Comparison of HII, HIII and THOR dummy responses with respect to PMHS sled tests. *Proceedings of IRCOBI Conference,* 2015, Lyon (France).

[9] Uriot et al. Investigations on the Belt-to-Pelvis Interaction in Case of Submarining. *Stapp Car Crash Journal*, 2006, Vol. 50, pp. 53-73.

[10] Hovenga et al. Rated facet hybrid-III 50th model with improved userfriendliness introduced. 10th International MADYMO Users Meeting, 2004, Amsterdam (Netherlands).

VIII. APPENDIX

Appendix 1: Description of the initial FE THOR dummy (Fig. 20)

Mass: 79.4383 kg
12 articulations
3 accelerometers
15 types of materials
297 materials for 3D elements
68 materials for 2D elements
50 materials for 1D elements
6 materials for discrete elements
6 materials for mass elements
7 materials for seatbelt elements

238861 nodes
524586 elements
453094 3D elements
71143 2D elements
117 1D elements
6 discrete elements
6 mass elements
22 nodes linked rigidly
314266 rigid elements
210320 deformable elements
428 parts

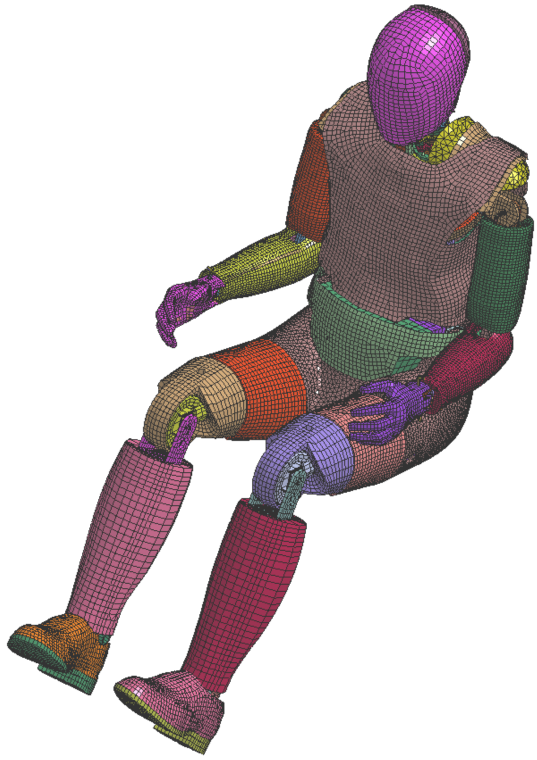

Fig. 20. FE THOR dummy.

The time step was imposed to 0.63 µs by a mass scaling. The added mass at the initial step was 157.65 g, 0.2% of the total mass.

Description of the elements

All the dummy parts were present within the model. The steel and aluminium parts were modelled with rigid bodies. The foam- and rubber-type materials (spine, neck, etc.) were modelled with deformable elements. The rigid elements were mainly used for the frame of the model (Fig. 21).

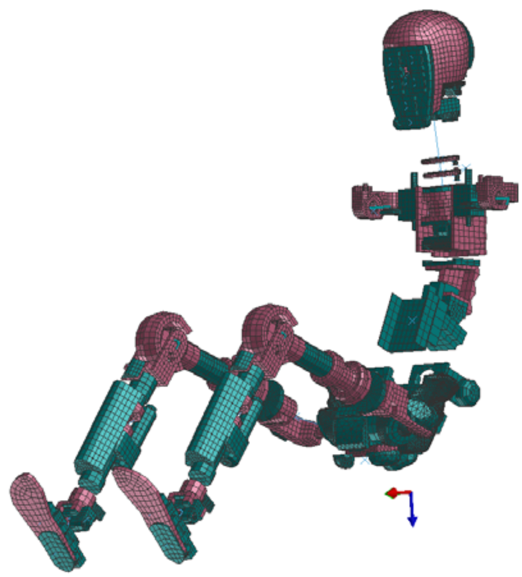

Fig. 21. Rigid frame of the FE THOR dummy.

Three types of rubber materials were used within this model (Fig. 22):
- MAT_SIMPLIFIED_RUBBER/FOAM (Type 181);
- MAT_SIMPLIFIED_RUBBER_WITH_DAMAGE (Type 183);
- MAT_BLATZ-KO_RUBBER (Type 007).

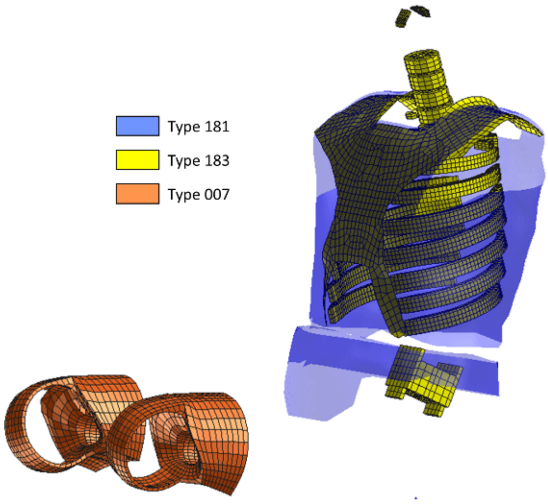

Fig. 22. Rubber-type materials.

Two types of foam materials were used with this model (Fig. 23):
- MAT_FU_CHANG_FOAM (type 083);
- MAT_LOW_DENSITY_FOAM (type 057).

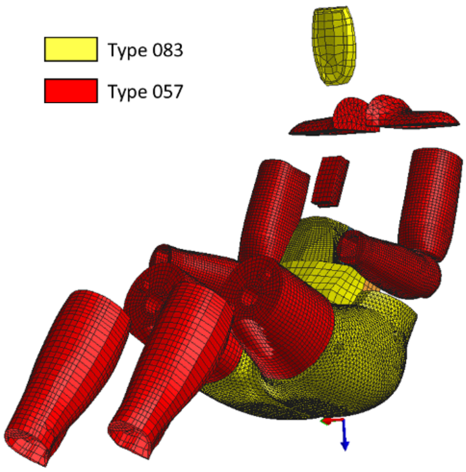

Fig. 23. Foam type materials.

In the V1 version, the upper arms were put in a rigid body in order to improve the calculation duration.

Appendix 2: Velocity (Fig. 24) and acceleration (Fig. 25) used for the different sled tests

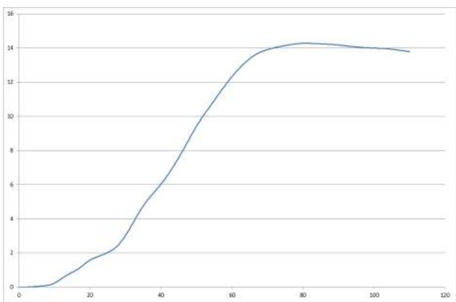

Fig. 24. Velocity ($m.s^{-1}$) used for the 9 PMHS tests.

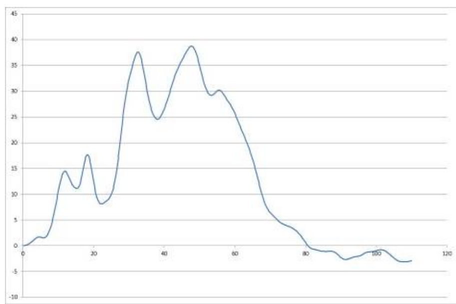

Fig. 25. Acceleration (g) used for the 9 PMHS tests.

Appendix 3: Parameters used and configurations tested during the FE sensitivity study

	Load limitation				Pretension		
Iteration Number	Shoulder load limitation 6 kN	Shoulder load limitation 4 kN	External lap-belt load limitation 6 kN	Internal lap-belt load limitation (Buckle) 4 kN	Retractor (3kN)	Belt buckle (3kN)	External lap-belt (3kN)
1	X				X		
2		X			X		
3	X					X	
4		X				X	
5	X					X	X
6	X		X		X		
7	X		X			X	
8	X		X			X	X
9		X	X		X		
10		X	X			X	
11		X	X			X	X
12		X	X	X		X	X
13	X			X		X	X
14		X		X		X	X

Appendix 4: Comparison between PMHS results and FE THOR dummies

T1 acceleration (m/s²): PMHS vs. FE dummies

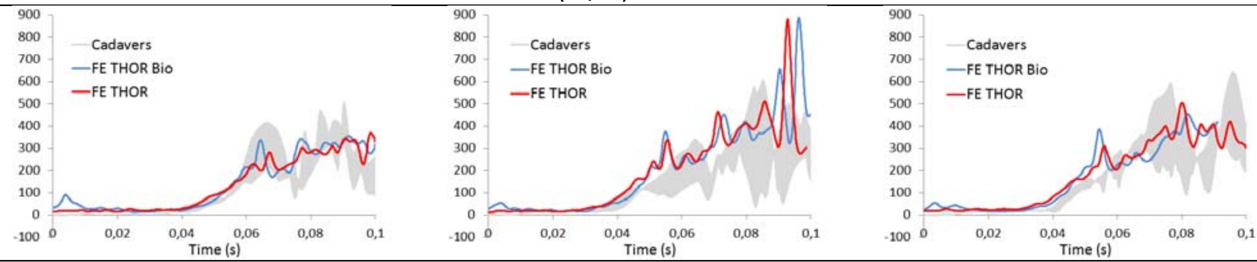

Configuration 1 Configuration 2 Configuration 3

Pelvis acceleration (m/s²): PMHS vs. FE dummies

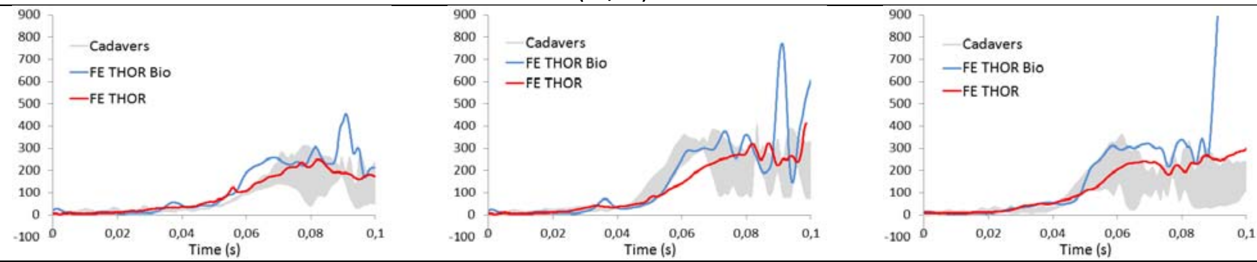

Configuration 1 Configuration 2 Configuration 3

Pelvis x displacement (m): PMHS vs. FE dummies

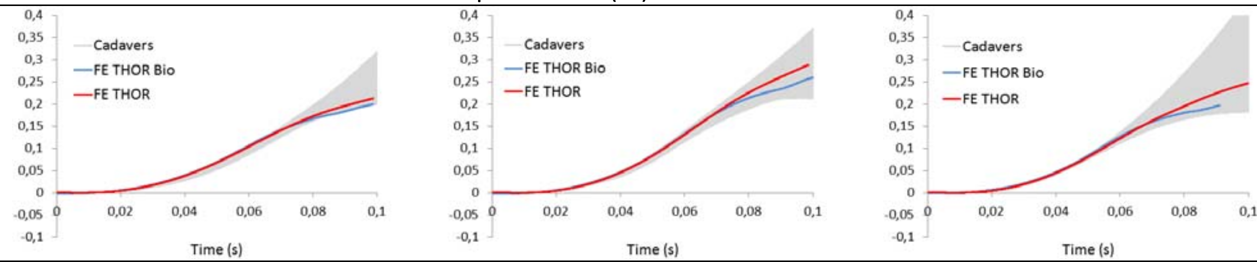

Configuration 1 Configuration 2 Configuration 3

External lap-belt force (N): PMHS vs. FE dummies

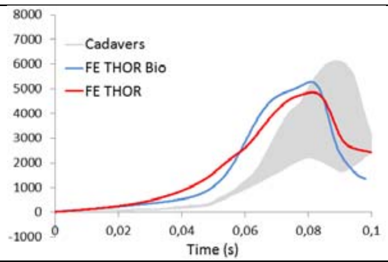

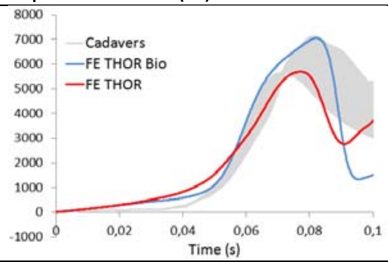

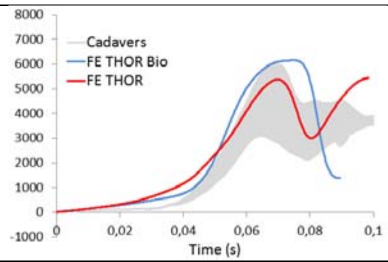

Configuration 1	Configuration 2	Configuration 3

Shoulder-belt force (N): PMHS vs. FE dummies

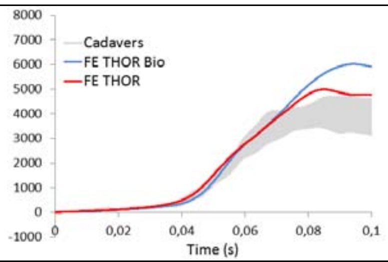

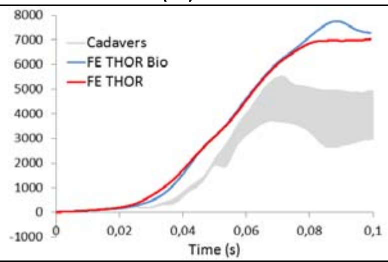

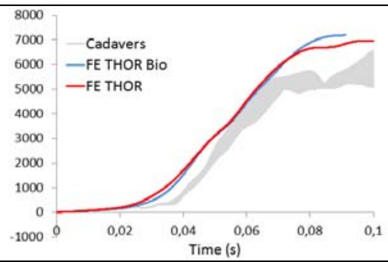

Configuration 1	Configuration 2	Configuration 3

Appendix 5: Model evaluation including Peak criterion, Peak timing criterion and WIFac criterion

Model reference	Channel	Peak criterion	Peak timing criterion	WIFac criterion	Total score
IRIS 30	Lap-belt force	79%	100%	78%	83%
IRIS 30	Shoulder-belt force	91%	100%	78%	86%
IRIS 30	Pelvis x displacement	97%	100%	92%	95%
IRIS 30	Pelvis acceleration	89%	96%	73%	83%
IRIS 30	Crossmember x disp.	97%	95%	84%	90%
IRIS 30	Crossmember z disp.	94%	100%	85%	91%
IRIS 31	Lap-belt force	87%	96%	84%	88%
IRIS 31	Shoulder-belt force	98%	100%	83%	90%
IRIS 31	Pelvis x displacement	94%	100%	90%	93%
IRIS 31	Pelvis acceleration	98%	91%	76%	85%
IRIS 31	Crossmember x disp.	85%	95%	73%	82%
IRIS 31	Crossmember z disp.	85%	100%	77%	84%
IRIS 32	Lap-belt force	99%	94%	77%	86%
IRIS 32	Shoulder-belt force	99%	96%	88%	93%
IRIS 32	Pelvis x displacement	82%	95%	76%	83%
IRIS 32	Pelvis acceleration	94%	96%	85%	90%
IRIS 32	Crossmember x disp.	97%	93%	84%	90%
IRIS 32	Crossmember z disp.	77%	99%	76%	80%
IRIS 33	Lap-belt force	85%	95%	73%	82%
IRIS 33	Shoulder-belt force	97%	68%	90%	80%
IRIS 33	Pelvis x displacement	86%	94%	83%	87%
IRIS 33	Pelvis acceleration	96%	83%	76%	83%
IRIS 33	Crossmember x disp.	82%	99%	70%	80%
IRIS 33	Crossmember z disp.	76%	90%	71%	77%
IRIS 34	Lap-belt force	95%	100%	80%	88%
IRIS 34	Shoulder-belt force	98%	95%	83%	90%
IRIS 34	Pelvis x displacement	86%	95%	79%	85%
IRIS 34	Pelvis acceleration	98%	95%	80%	88%
IRIS 34	Crossmember x disp.	99%	93%	86%	91%
IRIS 34	Crossmember z disp.	78%	96%	75%	81%
IRIS 39	Lap-belt force	95%	91%	56%	74%
IRIS 39	Shoulder-belt force	90%	88%	68%	79%
IRIS 39	Pelvis x displacement	47%	71%	38%	50%
IRIS 39	Pelvis acceleration	82%	91%	48%	68%
IRIS 39	Crossmember x disp.	73%	90%	80%	80%
IRIS 39	Crossmember z disp.	56%	80%	46%	58%
IRIS 40	Lap-belt force	88%	93%	87%	89%
IRIS 40	Shoulder-belt force	92%	72%	89%	82%
IRIS 40	Pelvis x displacement	62%	90%	70%	71%
IRIS 40	Pelvis acceleration	52%	94%	55%	62%
IRIS 40	Crossmember x disp.	67%	93%	78%	77%
IRIS 40	Crossmember z disp.	81%	91%	77%	82%
IRIS 41	Lap-belt force	98%	92%	43%	67%
IRIS 41	Shoulder-belt force	100%	88%	74%	83%
IRIS 41	Pelvis x displacement	54%	68%	49%	56%
IRIS 41	Pelvis acceleration	74%	89%	42%	63%
IRIS 41	Crossmember x disp.	69%	96%	77%	78%
IRIS 41	Crossmember z disp.	48%	80%	38%	52%